Quantitative Reverse Transcription-Polymerase Chain Reaction Detection of Cytokeratin 20 in Noncolorectal Lymph Nodes[1]

Richie Soong,[2] Kurt Beyser, Oliver Basten, Andreas Kalbe, Josef Rueschoff, and Karim Tabiti

Roche Diagnostics GmbH, 82377 Penzberg [R. S., A. K., K. T.]; Klinikum Kassel, 34041 Kassel [K. B., J. R.]; and Klinikum Fulda, 36001 Fulda [O. B.], Germany

ABSTRACT

Purpose: **Unexpected reverse transcription-PCR detection of *cytokeratin 20* (*CK20*) in samples from healthy individuals and cancer types not expected to express *CK20* has cast uncertainty on the role of *CK20* as a specific marker of disseminated colorectal cells. We aimed to clarify the specificity of *CK20* by examining its expression profile by real-time reverse transcription-PCR.**

Experimental Design: **A quantitative real-time PCR assay on the LightCycler instrument was developed and used to examine *CK20* expression in tumors and lymph nodes from subjects with colorectal and breast carcinoma, head and neck and vulval squamous cell carcinoma, and melanoma. To select a method for reproducible quantification, four approaches were evaluated.**

Results: **The developed assay allowed rapid, convenient-to-use, specific, sensitive, and reproducible *CK20* quantification amenable to large-scale analysis. For quantity calculation, an efficiency-adjusted relative ratio method was selected that controls for RNA loading and integrity as well as inefficient PCR reactions and provides a platform for standardization across laboratories. Using this assay, we detected *CK20* in 41 of 89 (46%) lymph nodes from noncolorectal cancer types. There was a strong association between *CK20* detection and lymph node metastasis determined by histology ($P < 0.0001$). Quantitatively, *CK20* expression levels in colorectal cancer lymph nodes significantly exceeded the levels obtained in lymph nodes of extracolonic carcinomas ($P < 0.05$). Mean *CK20* levels in lymph nodes and tumors from subjects with colorectal and breast cancers were similar in a tumor-type specific fashion.**

Conclusions: **These results characterize low-level, epithelial cell-specific *CK20* expression in infiltrated lymph nodes from subjects with noncolorectal cancer types and demonstrate the potential advantages of detecting circulating epithelial cells by quantitative PCR.**

INTRODUCTION

Despite the histopathological diagnosis of tumor-free margins, many cancer patients suffer a recurrence of their disease (1). One belief is that these recurrences may arise from residual disseminated tumor cells (also termed "micrometastasis" or "minimal residual disease") that at present are undetectable by conventional methods (2). The detection of these cells by molecular techniques could impact greatly on future patient management and therapy; this option has driven a growing field of research in recent years (3). The majority of studies rely on the principle of detecting a target of restricted expression in an extraneous environment. In many cases, this has taken the form of detecting tissue- or tumor-specific molecular markers in compartments of potential dissemination, such as blood, lymph nodes, and bone marrow.

CK20[3] is a member of the intermediate filament protein family involved in cell structure and differentiation (4, 5). Early immunological and Northern blot studies found that *CK20* expression was restricted primarily to gastrointestinal tissue, transitional cell carcinoma, and Merkel cells (4–6). Other adenocarcinomas, such as those from breast, endometrium, and lung, as well as squamous cell carcinomas were found not to express *CK20*. This restricted expression profile has formed the basis of many studies examining blood, lymph nodes, bone marrow, and urine for *CK20* as a surrogate marker for disseminated tumor cells.

In recent years, many studies have taken advantage of the increased sensitivity of PCR assays to detect *CK20* at levels previously undetectable by conventional molecular methods. However, these studies have produced many controversial findings. Whereas some studies have found associations between *CK20* and stage (7–9), grade (10), and recurrence (8), others have not (11, 12). Critically, although some studies have reported specific *CK20* detection (7, 13–20), others have detected *CK20* in blood, bone marrow, and urine from healthy donors or patients with nonmalignant disease (11, 12, 20–23). A further confounding factor has been the recent detection of *CK20* in samples from breast (13, 20, 24, 25), thyroid (19), endometrial (26, 27), lung (14), and pancreas (8, 14, 20) carcinoma and oral squamous cell carcinoma (16), although the reasons for this unexpected *CK20* detection have not been examined. Together, these discrepancies have made it difficult to interpret the relevance of detecting circulating epithelial cells by *CK20* RT-PCR.

One source of this uncertainty is that few studies have

Received 4/3/01; revised 7/9/01; accepted 8/2/01.

The costs of publication of this article were defrayed in part by the payment of page charges. This article must therefore be hereby marked *advertisement* in accordance with 18 U.S.C. Section 1734 solely to indicate this fact.

[1] This study was supported financially by Roche Diagnostics GmbH, Penzberg, Germany.

[2] To whom requests for reprints should be addressed, at Roche Diagnostics GmbH, Nonnenwald 2, 82377 Penzberg, Germany. Phone: 49 8856 605124; Fax: 49 8856 603180; E-mail: Richie.Soong@roche.com.

[3] The abbreviations used are: CK20, cytokeratin 20; RT-PCR, reverse transcription-PCR.

Table 1 Frequency of *CK20* detection in lymph nodes with and without epithelial cell invasion (according to histology)

Cancer type	Without epithelial cell invasion, *n* (%)	With epithelial cell invasion, *n* (%)	Total, *n* (%)
Colorectal	NA[a]	9/9 (100%)	9/9 (100%)
Noncolorectal	2/44 (5%)	39/45 (87%)	41/89 (46%)
Breast	0/15 (0%)	6/6 (100%)	6/21 (29%)
Melanoma	1/13 (8%)	NA	1/13 (8%)
Head and neck SCC	1/13 (8%)	30/35 (86%)	31/48 (65%)
Vulva SCC	0/3 (0%)	3/4 (75%)	3/7 (43%)

[a] NA, none analyzed; SCC, squamous cell carcinoma.

addressed the expression profile of *CK20* mRNA detectable by PCR. A major reason for this has been the lack of standardized, quantitative PCR assays available for large-scale analysis. In recent years, the development of real-time, on-line fluorescence-monitoring PCR technology has promised to bring reliable and accurate PCR quantification (28). This technology monitors the entire PCR reaction by fluorescence detection, thereby allowing the beginning of the exponential phase of amplification (so-called "crossing points" or "threshold cycle") to be measured. This reaction point is considered the most reliable point of the PCR reaction related to sample concentration (29). However, although the number of studies using this approach is increasing, few have examined the factors affecting the interpretation of results obtained by real-time PCR, and suitable approaches for quantification are yet to be established.

To clarify the expression profile and specificity of *CK20* RT-PCR detection, we sought to compare *CK20* levels in a collection of lymph nodes and tumors from various cancer types by quantitative PCR. To ensure correct interpretation, we developed a standardizable, quantitative real-time PCR assay and a quantification concept for high reproducibility and investigated factors influencing results obtained from these assays.

MATERIALS AND METHODS

Sample Material. Ten colorectal and 11 breast tumors as well as 98 lymph nodes from various cancer types were collected from subjects undergoing surgery for their disease at Klinikum Kassel during 1999. The types and numbers of lymph nodes examined and their metastatic status are displayed in Table 1. Lymph nodes were assessed for metastases by routine histology after conventional H&E staining. For RNA extraction, 30–240 mg of tissue was added to 1 ml of TriPure Reagent (Roche Diagnostics, Mannheim, Germany) and homogenized with an Ultra-Turrax T25 homogenizer (IKA-Labortechnik, Staufen, Germany). RNA was extracted from the homogenate according to the manufacturer's protocol and measured spectrophotometrically at 260 nm.

Cell Lines. The HT29 colon carcinoma cell line (American Type Culture Collection, Manassas, VA) was grown and maintained in DMEM with 0.9% glucose, and the HL60 promyelocytic leukemia cell line (American Type Culture Collection) was grown and maintained in RPMI 1640. Both cell lines were supplemented with 10% FCS and 1% (v/v) 2 mM glutamine and incubated at 37°C in 5% carbon dioxide in a humidified chamber. Five HT29 cell suspensions (100 μl) containing 10^4, 10^3, 10^2, 10, and 0 cells, respectively, in 1× PBS were each mixed with 100 μl of 10^6 HL60 cells. The entire 200 μl was loaded onto columns from the HighPure RNA Isolation Kit, and RNA was extracted according to the manufacturer's instructions. All reagents were from Roche Diagnostics (Mannheim, Germany) unless specified.

cDNA Preparation. cDNA was produced in a 20-μl reaction from 500 ng of tissue RNA or 10 μl of a 100-μl cell line RNA eluate. The other components were 20 units of AMV reverse transcriptase, 1× AMV reaction buffer, 10 mM deoxynucleotide triphosphates, and 3.2 μg of random hexamers. The reactions were incubated at 25°C for 10 min, 42°C for 1 h, and 94°C for 5 min. All reagents were from Roche Diagnostics.

LightCycler PCR. Each reaction contained 2 μl of cDNA, 1× Detection Mix, and 1× DNA Master Hybridization Probes Mix (Roche Diagnostics) in a 20-μl volume. For the amplification of *CK20* and the housekeeping gene, *porphorynbilinogen deaminase (PBGD*), separate detection mixtures were made. Each 10× Detection Mix included 5 μM each primer (forward and reverse), 2 μM each hybridization probe (fluorescein and LC-Red640), and 40 mM $MgCl_2$. The forward and reverse PCR primers for *CK20* were placed in exons 1 and 2, respectively, amplifying a 125-bp amplicon, and those for *PBGD* were in exon 1 and 3, respectively, giving a 151-bp amplicon. One of the two hybridization probes for *CK20* spanned the exon 1/2 boundary, whereas one for *PBGD* spanned the exon 2/3 boundary to ensure detection of only mRNA sequences. We cannot reveal the primer and hybridization probe sequences because of patent restrictions; however, all of the components used in this assay can be readily found in a commercially available kit (Roche Diagnostics).

In the LightCycler instrument, each reaction capillary underwent a 1-min incubation at 94°C before 50 cycles of 94°C for 0 s, 60°C for 10 s, and 72°C for 5 s. The PCR run was concluded with a 40°C incubation for 30 s. Fluorescence was monitored at the conclusion of each 60°C incubation. The PCR reactions for *CK20* and *PBGD* were conducted in separate capillaries. The fluorescence detected in channel F2/F1 was analyzed by the LightCycler Analysis Software at the end of the run. The crossing points (beginning of the PCR exponential phase) for each reaction were determined by the Second Derivative Maximum algorithm and arithmetic baseline adjustment. For size estimation, amplified product was examined on 2% agarose gels with 1 mg/ml ethidium bromide (Roth, Karlsruhe, Germany) with a 100-bp DNA molecular weight marker XIV ladder (Roche Diagnostics).

PCR Quantification. Four methods for quantification were evaluated. The first two methods used a standard curve. Partial DNA fragments of *CK20* and *PBGD* were amplified and cloned into separate pSPTBM21 cloning vectors (Roche Diagnostics). After linearization, the copy numbers were estimated by spectrophotometry with the assumption that 1 mol represents 6×10^{23} molecules. Dilution series containing 10^2, 10^3, 10^4, and 10^5 copies were used as PCR templates to construct a standard curve based on the relationship between the crossing point and the logarithm of copy number. Separate standard curves for *CK20* and *PBGD* were included in each PCR run. In all cases, the correlation coefficient for the curves was -1. From this linear relationship, the copy numbers were calculated from the standard curve and crossing points of each sample. The first quantification method calculated the copy numbers of *CK20* per ng of RNA. The second method calculated a *CK20* relative ratio, namely the ratio of *CK20* to *PBGD* copies in a sample relative to *CK20* to *PBGD* copies in a calibrator sample. The calibrator was 10 ng/μl RNA from the HT29 colorectal carcinoma cell line and was included with each RT-PCR run. The final result was multiplied by 1,000,000, setting the calibrator in each run to this value. Therefore, a sample with a ratio of 100,000 had 10 times less *CK20* than the calibrator.

For the third and fourth methods, the calculation of the *CK20* relative ratio did not require a standard curve, but instead was a function of the PCR reaction efficiency and the crossing points of *CK20* and *PBGD* of the unknown and calibrator samples. For the third method, the *CK20* relative ratio was calculated assuming a reaction efficiency of 2, which corresponded to a perfect doubling of PCR product with each cycle according to the following equation:

$$2^{[\mathrm{CP}(CK20.\mathrm{C})-\mathrm{CP}(CK20.\mathrm{U})]-[\mathrm{CP}(PBGD.\mathrm{C})-\mathrm{CP}(PBGD.\mathrm{U})]} \times 1{,}000{,}000 \quad \text{(A)}$$

where CP is the crossing point; U is the unknown sample, and C is the calibrator.

For the fourth method, because PCR product in some reactions does not precisely double with each cycle, adjusted *CK20* and *PBGD* efficiencies for the calculation of the relative ratio were used. The efficiency was calculated as $10^{-1/\mathrm{slope}}$, where the slope of the line was determined from the relationship between the PCR crossing point and the logarithm of concentration. The adjusted *CK20* and *PBGD* efficiencies were the mean efficiencies determined from seven individual tissue samples diluted over four 10-fold different concentrations. The mean efficiencies were 2.115 (± 0.029) for *CK20* and 2.101 (± 0.141) for *PBGD* and were used for the calculation of the *CK20* relative ratio of the tissue samples. With these efficiencies, the relative ratio was calculated according to the following equation:

$$\frac{\mathrm{Efficiency}\ (CK20)^{\mathrm{CP}(CK20.\mathrm{C}-CK20.\mathrm{U})}}{\mathrm{Efficiency}\ (PBGD)^{\mathrm{CP}(PBGD.\mathrm{C}\ -\ PBGD.\mathrm{U})}} \times 1{,}000{,}000 \quad \text{(B)}$$

This fourth method was selected for the quantification of tissue samples.

Statitsical Analysis. To evaluate the reproducibility of the quantities derived from each quantification method, the coefficient of variation, which calculates the percentage of the SD of a data series to its mean, was determined. The association between *CK20* detection in noncolorectal lymph nodes and epithelial invasion determined histologically was examined using the χ^2 test. Differences between the mean *CK20* quantities in lymph nodes from subjects with colorectal and noncolorectal cancers were tested for by a two-tailed *t* test. All calculations were performed using Excel 97 (Microsoft, Seattle, WA).

RESULTS

Development of a Quantitative *CK20* LightCycler PCR Assay. A protocol for the quantification of *CK20* using the real-time PCR LightCycler instrument was developed. For the analysis of each sample, a single aliquot of RNA underwent a two-step RT-PCR procedure with random hexamers used for RNA priming. Aliquots from the same cDNA sample were subjected to real-time PCR for *CK20* and *PBGD* in separate capillaries, and their crossing points were measured by the LightCycler software and used for quantification. Accompanying the samples in each RT-PCR run was a calibrator sample comprising RNA from HT29 cells, whose *CK20* and *PBGD* crossing points were also measured for quantification.

All RT-PCR reaction reagents and concentrations used in this protocol were selected after rigorous optimization experiments. Where possible, reagents were combined in mixed solutions to minimize the number of manipulations. The LightCycler hybridization probes format was selected to provide an additional level of specificity and to allow fluorescent monitoring of the PCR kinetic reaction (29). Primers and hybridization probes for *CK20* and *PBGD* were designed to amplify and detect short amplicons spanning exon-intron boundaries, thereby allowing reduction of cycling times and preventing the detection of genomic DNA. As a reference gene, after testing a variety of housekeeping genes (results not shown) we selected *PBGD* because of its relatively low expression and lack of pseudogenes. With the rapid cycling capabilities of the LightCycler instrument (30), the total run time for the reverse transcription (45 min) and PCR (30 min) steps was 75 min.

Sensitivity and Specificity. In plasmid dilution experiments, concentrations down to 1 copy of *CK20* or *PBGD* was detectable by this assay (Fig. 1). *CK20* could be detected in HT29 cells to a dilution of 10 cells mixed with 10^6 HL60 cells, whereas no signal was detected from 10^6 HL60 cells alone (Fig. 1). Agarose gel electrophoresis, sequencing, and LightCycler melting curve analysis of the amplified fragments showed the correct size (Fig. 1), sequence, and melting pattern, respectively (results not shown).

Quantification Concept Reproducibility. We assessed the reproducibility of the four methods for quantifying *CK20* (see "Materials and Methods"), using a single tissue sample in a total of 27 replicates for each method, involving 3 serial dilutions, 3 separate reverse transcriptions, and 9 individual PCR assays (Table 2). The coefficient of variation from the first method, which determined absolute *CK20* copy number per ng of RNA via a plasmid-derived standard curve, was 43%. For the second method, which also used a standard curve but calculated a relative *CK20* ratio, the coefficient of variation was 32%. The coefficient of variation for the slope of the standard curve from

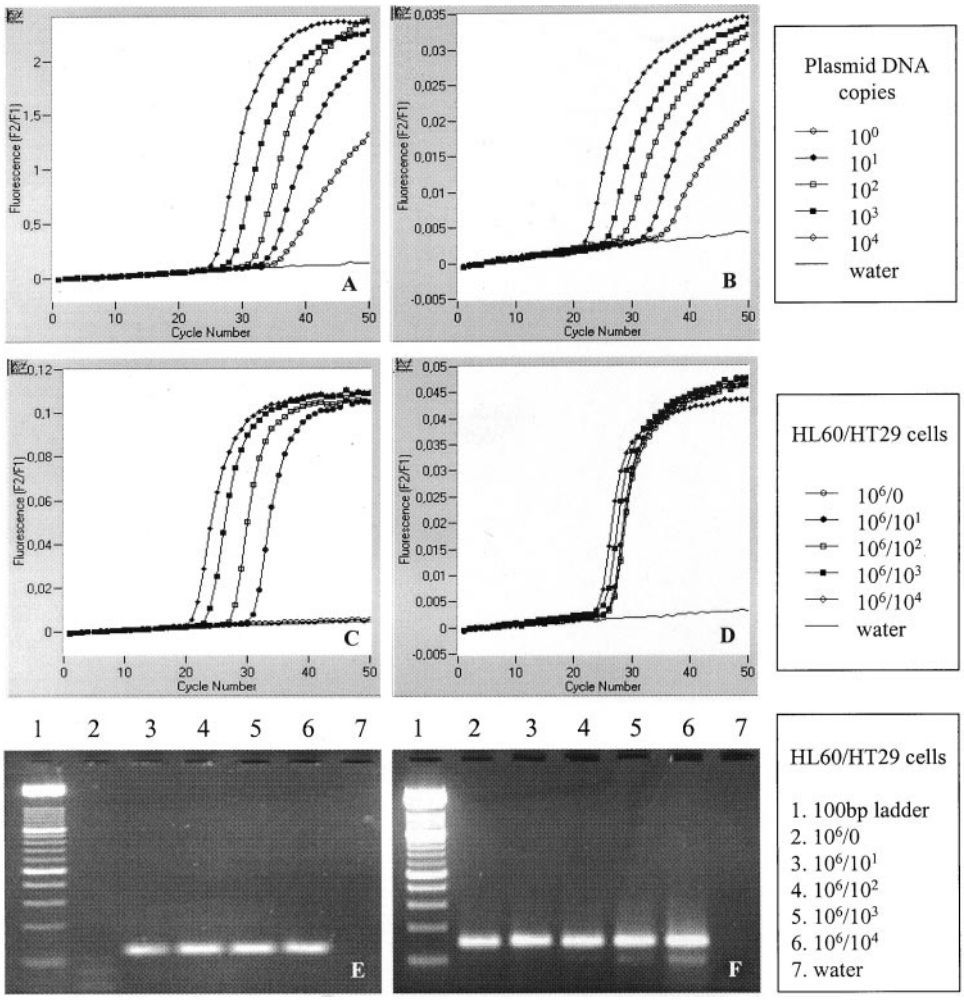

Fig. 1 Sensitivity of the *CK20* RT-PCR assay. Real-time PCR (*A–D*) and agarose gel electrophoresis (*E* and *F*) detection of *CK20* (*A*, *C*, and *E*) and *PBGD* (*B*, *D*, and *F*) in plasmid DNA (*A* and *B*) and HT29 colorectal cells with a HL60 promyeloleukemic cell background (*C–F*).

Table 2 Reproducibility of the *CK20* relative ratio

All values expressed as mean (coefficient of variation).

	Amount of RNA				
	Calibrator (10 ng; $n = 9$)[a]	Sample			
		1 ng ($n = 9$)	10 ng ($n = 9$)	100 ng ($n = 9$)	All ($n = 27$)
CK20 crossing point	24.69 (0.5%)	28.09 (1.2%)	25.05 (1.0%)	22.80 (0.7%)	
PBGD crossing point	26.72 (0.4%)	30.55 (0.8%)	27.52 (0.9%)	25.18 (0.7%)	
CK20 copy number	15,441 (17%)	1452 (30%)	11,982 (18%)	58,159 (15%)	
PBGD copy number	1763 (13%)	213 (26%)	1134 (13%)	4131 (9%)	
CK20 copies/ng RNA (Standard curve)	154 (17%)	1452 (30%)	1198 (18%)	581 (15%)	1077 (43%)
CK20 relative ratio (Standard curve)	1,000,000	787,135 (21%)	1,211,483 (12%)	1,616,892 (13%)	12,050,170 (24%)
CK20 relative ratio (Efficiency = 2)	1,000,000	1,360,699 (16%)	1,351,985 (9%)	1,286,643 (13%)	1,333,109 (12%)
CK20 relative ratio (Efficiency adjusted)	1,000,000	1,361,204 (17%)	1,378,494 (10%)	1,327,308 (14%)	1,355,669 (13%)

[a] *n*, number of determinations.

the nine PCR runs was 2.3% for *CK20* and 2.5% for *PBGD* the *Y*-intercept was 0.9% for *CK20* and 1.3% for *PBGD*. For the third method, which used an algorithm for calculation of the *CK20* relative ratio and assumed reaction efficiencies of 2, the coefficient of variation was 12%, whereas for the fourth method, which used adjusted individual efficiencies for the *CK20* and *PBGD* reactions, it was 13%.

***CK20* Detection Frequency.** Of the tumors analyzed, 10 of 10 (100%) colorectal and 8 of 11 (73%) breast carcinomas were *CK20* positive. The frequency of *CK20* detection in the

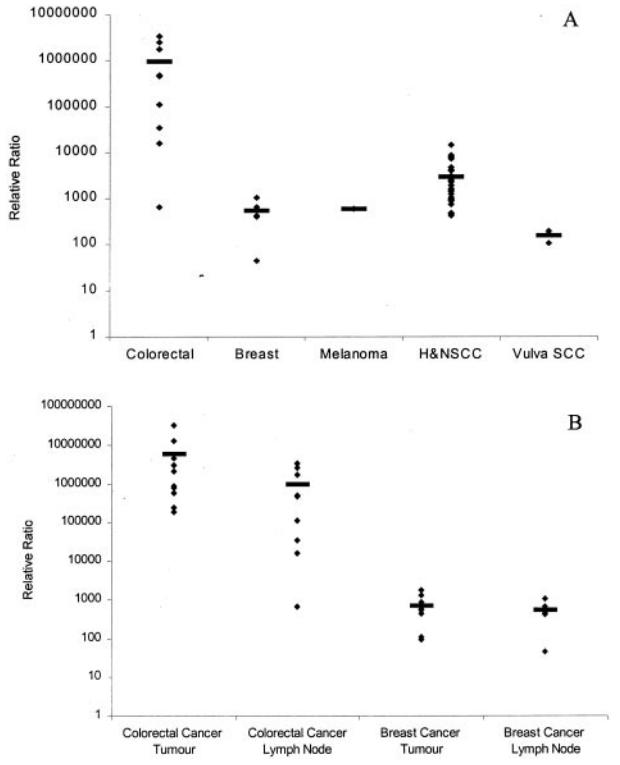

Fig. 2 Relative quantification of *CK20* in colorectal and noncolorectal samples. The mean relative ratios of the *CK20*-positive samples are indicated by a *horizontal bar*. *A*, comparison of *CK20* levels in lymph nodes from colorectal and noncolorectal cancer types. *H&N*, head and neck, *SCC*, squamous cell carcinoma. *B*, comparison of *CK20* levels between lymph nodes and tumors from patients with breast and colorectal cancer.

different types of lymph node samples is summarized in Table 1. All 9 (100%) colorectal lymph nodes examined were *CK20* positive, whereas 41 of 89 (46%) noncolorectal lymph nodes had detectable *CK20* mRNA. There was a strong correlation ($P < 0.0001$) between *CK20* detection and lymph node epithelial invasion in the noncolorectal lymph nodes.

***CK20* Quantity.** In lymph nodes with detectable *CK20* mRNA, the mean relative *CK20* quantity was significantly higher in colorectal than in noncolorectal specimens ($P < 0.05$; Fig. 2*A*). Comparison of the mean *CK20* relative ratio between tumors and lymph nodes showed similar relative levels according to tissue type (Fig. 2*B*). Mean *CK20* levels in tumor and lymph nodes were both relatively high in colorectal and both low in breast carcinoma samples.

DISCUSSION

A major obstacle to accurately evaluating the clinical relevance of detecting circulating epithelial cells by *CK20* RT-PCR has been the underlying uncertainty over its expression profile and specificity. We sought to clarify this uncertainty by measuring *CK20* levels in a collection of lymph nodes and tumors from subjects with a range of cancer types by quantitative PCR.

One factor contributing to the uncertainty about *CK20* has been the lack of standardizable, quantitative assays amenable to large-scale analysis for its assessment. The majority of previous assays have often involved nested conventional PCR followed by detection through visualization on agarose gels (7–27), requiring long analysis times and providing only a limited qualitative analysis. Two competitive PCR assays for *CK20* quantification have been described (31, 32); however, the many manipulations required for these assays make them difficult to apply to a large-scale analysis. A third assay using real-time PCR technology has also been reported; however, it detected *CK20* in 100% of blood samples from healthy donors (21), creating uncertainty over its specificity.

An essential part of this study was the development of a convenient and reliable protocol for *CK20* quantification using real-time PCR technology. Numerous design elements have been selected and optimized to provide controls for influencing factors and to facilitate standardizable and large-scale analysis. Rapid analysis times, including 30 min for the PCR, were made possible through the use of the LightCycler instrument, which has rapid cycling thermodynamics (30), and the selection of short amplicons. Convenience has been enhanced by combining reagents and applying a nonnested PCR procedure. Along with the LightCycler closed capillary system, reducing the number of manipulations also minimizes the risk of cross-contamination. Selection of a two-step RT-PCR procedure enables conservation of samples with multiple PCR analyses possible from a single RNA aliquot. Random hexamer priming for the reverse transcription step has been selected to provide flexibility to sample sources.

In addition to the reduction of cross-contamination, other design elements help to ensure specificity. Selection of the LightCycler hybridization probes format means that amplification and detection of *CK20* and *PBGD* occurs only after the annealing of four sequence-specific oligonucleotides. These PCR primers and hybridization probes have been positioned to span exon-intron boundaries, reducing the risk of detecting genomic DNA. Agarose gel electrophoresis, sequencing, and LightCycler melting curve analysis of the amplified fragments consistently showed the correct size (Fig. 1), sequence, and melting pattern (results not shown) of the amplicons. The sensitivity of this assay is comparable to those reported previously (15, 21, 31), allowing the detection of 1–10 plasmid copies of *CK20* and *PBGD* and of 10 plasmid copies of HT29 colorectal cells in a background of 10^6 HL60 promyeloleukemic cells (Fig. 1).

As with assay design, the method of translating crossing points into a quantitative result can have a significant impact on data interpretation. After careful consideration of numerous methods, we selected a method that calculates a relative ratio of *CK20* levels with an adjusted efficiency. The final result obtained by this method is a ratio of *CK20* to *PBGD* in a sample relative to the ratio of *CK20* to *PBGD* in a calibrator. The calculation of *PBGD* levels adjusts for RNA loading and integrity within the PCR run. This makes it a more relevant normalizer than spectrophotometric assessment and obviates the requirement to estimate sample concentrations prior to PCR analysis. The analysis of calibrator RNA in each run provides adjustment for inter-PCR variations and also sets a standard reference point. Additionally, efficiency values adjusted for *CK20* and *PBGD* were used for the calculation of the relative

ratio to account for differences in efficiency between the two reactions. Together these methods provide a quantification amount that allows for direct comparison of *CK20* levels while adjusting for factors that may influence quantity determination.

To assess the suitability of this calculation method, we measured its reproducibility on 27 replicates of a sample and compared it with three alternative calculation methods (Table 2). The 27 determinations involved analysis over three different concentrations, three reverse transcription steps, and nine separate PCR reactions. The coefficients of variation for the current method using adjusted efficiencies and one using an assumed perfect efficiency of 2 were 13% and 12%, respectively, demonstrating the high reproducibility and the robustness of these methods to RNA loading. In this study, we favored the adjusted efficiency method because it would be more effective in the event of inefficient PCR reactions. The similarity of *CK20* and *PBGD* reaction efficiencies makes the effect of this adjustment difficult to demonstrate; nevertheless, this result suggests that either method could be used with similar reproducibility for this *CK20* assay. The variation for both approaches was lower than the coefficient of variation of 32% for the *CK20* relative ratio obtained by a standard curve method. A major contributing factor to this lower reproducibility was the error introduced by the minor variations of the slope and *Y*-intercept of the standard curve between PCR runs. Furthermore, the coefficient of variation was 43% for a method that determines absolute copy numbers per ng of RNA via a standard curve, without factoring *PBGD* quantities and a calibrator ratio, which demonstrates the potential pitfalls of spectrophotometric RNA measurement and lack of calibration between RT-PCR runs.

Recent studies have found *CK20* expression in samples from breast (13, 20, 24, 25), thyroid (19), endometrial (26, 27), pancreas (8, 14, 20), and oral squamous cell carcinomas (16), although these cancer types are not expected to express *CK20*. To explore this discrepancy, we used our quantitative PCR assay to compare *CK20* expression levels in lymph nodes from subjects with colorectal cancer with those from subjects with a collection of noncolorectal cancers, namely breast, head and neck, and vulva squamous cell carcinoma and melanoma. We were surprised to find *CK20* expression in lymph nodes from all of the noncancer types examined (Table 1), which suggests that *CK20* expression may not be as restricted as previously thought. Four studies, including ours, have detected *CK20* in samples from breast carcinoma (13, 20, 24, 25); however, this is the first report of *CK20* in samples from head and neck and vulva squamous cell carcinoma and melanoma.

We examined *CK20* expression levels in lymph nodes from subjects with noncolorectal cancer and observed extremely low levels relative to the expression in lymph nodes from subjects with colorectal cancer. The difference in *CK20* levels between the highest quantity in a colorectal cancer lymph node (32,997,451) and the lowest quantity in a breast cancer lymph node (45) was ~700,000-fold (Fig. 2*A*). When we compared levels between lymph nodes and tumors from subjects with colorectal and breast cancer, we found similar quantitative differences (Fig. 2*B*), which suggests that this result was not an artifact of lymph node analysis. *CK20* levels were high in both lymph nodes and tumors from subjects with colorectal cancer and low in both lymph nodes and tumors from subjects with breast cancer. This result provides proof of large quantitative differences in *CK20* expression detectable by quantitative PCR and may help to provide a possible explanation for discrepant observations of the *CK20* expression profile. With these quantitative differences, less sensitive assays would be able to detect expression only in samples from colorectal cancers, whereas those more sensitive would detect *CK20* in a larger range. To our knowledge, the expression profile of *CK20* has been defined primarily by Northern blot and immunohistochemical analyses (5, 6). This result demonstrates that assumptions about expression profiles obtained by alternative methods should be interpreted with caution.

One possible explanation for *CK20* detection in these cancer types is nonspecificity; however, we believe that this is highly unlikely. Along with assay design elements for specificity, a strong association was observed between *CK20* detection and lymph node metastases demonstrated by histology (Table 1). Of the lymph nodes from noncolorectal cancer types, *CK20* was detected in 87% (39 of 45) of cancer metastases and only 5% (2 of 44) of lymph nodes without histological evidence of metastatic infiltration.

The strong association between *CK20* detection and metastatic invasion also suggests that detection of *CK20* in lymph nodes may provide clinically relevant information in these tumor types. However, the small numbers of samples for each cancer type in this series prevents analysis of their association with other clinical parameters. Other studies in noninfiltrated lymph nodes from breast (13) and colorectal (18, 33, 34) cancer suggest that *CK20* detection may help to identify cancer cell dissemination at a more sensitive level than conventional means. Rosenberg *et al.* (34) recently observed a nonsignificant trend between *CK20* detection in lymph nodes from subjects with colorectal cancer and survival in a small sample series with a short follow-up time. Thus, further studies are clearly warranted to investigate the potential role of *CK20* detection in lymph nodes.

In summary, we have described the development of a standardizable, quantitative *CK20* PCR assay and have used this assay to characterize epithelial-specific, low-level *CK20* expression in cancer types not expected to express *CK20*. This result helps to clarify uncertainty over the expression profile of *CK20* and demonstrates the potential new information that quantitative PCR analysis may provide. Similar uncertainty surrounds the specificity of *CK20* in blood, bone marrow, and urine from healthy donors. The potential benefit of a quantitative PCR analysis of these sample types awaits further analysis.

REFERENCES

1. Deans, G. T., Parks, T. G., Rowlands, B. J., and Spence, R. A. J. Prognostic factors in colorectal cancer. Br. J. Surg., *79:* 608–613, 1992.

2. Ghossein, R. A., and Rosai, J., Polymerase chain reaction in the detection of micrometastasis and circulating tumor cells. Cancer (Phila.), *78:* 10–16, 1996.

3. Burchill, S. A., and Selby, P. J. Molecular detection of low level disease in patients with cancer. J. Pathol., *190:* 6–14, 2000.

4. Moll, R., Lowe, A., Laufer, J., and Franke, W. W. Cytokeratin 20 in human carcinomas. A new histodiagnostic marker detected by monoclonal antibodies. Am. J. Pathol., *140:* 427–447, 1992.

5. Moll, R., Zimbelmann, R., Goldschmidt, M. D., Keith, M., Laufer, J., Kasper, M., Koch, P. J., and Franke, W. W. The human gene encoding

cytokeratin 20 and its expression during fetal development and in gastrointestinal carcinomas. Differentiation, *53:* 75–93, 1993.

6. Miettinen, M. Keratin 20: immunohistochemical marker for gastrointestinal, urothelial, and Merkel cell carcinomas. Mod. Pathol., *8:* 384–388, 1995.

7. Funaki, N. O., Tanaka, J., Ohshio, G., Onodera, H., Maetani, S., and Imamura, M. Cytokeratin 20 mRNA in peripheral venous blood of colorectal carcinoma patients. Br. J. Cancer, *77:* 1327–1332, 1998.

8. Soeth, E., Vogel, I., Roder, C., Juhl, H., Marxsen, J., Kruger, U., Henne-Bruns, D., Kremer, B., and Kalthoff, H. Comparative analysis of bone marrow and venous blood isolates from gastrointestinal cancer patients for the detection of disseminated tumor cells using reverse transcription PCR. Cancer Res., *57:* 3106–3110, 1997.

9. Weitz, J., Kienle, P., Lacroix, J., Willeke, F., Benner, A., Lehnert, T., Herfarth, C., and von Knebel Doeberitz, M. Dissemination of tumor cells in patients undergoing surgery for colorectal cancer. Clin. Cancer Res., *4:* 343–348, 1998.

10. Rotem, D., Cassel, A., Lindenfeld, N., Mecz, Y., Sova, Y., Resnick, M., and Stein, A. Urinary cytokeratin 20 as a marker for transitional cell carcinoma. Eur. Urol., *37:* 601–604, 2000.

11. Wyld, D. K., Selby, P., Perren, T. J., Jonas, S. K., Allen-Mersh, T. G., Wheeldon, J., and Burchill, S. A. Detection of colorectal cancer cells in peripheral blood by reverse-transcriptase polymerase chain reaction for cytokeratin 20. Int. J. Cancer, *79:* 288–293, 1998.

12. Buchumensky, V., Klein, A., Zemer, R., Kessler, O. J., Zimlichman, S., and Nissenkorn, I. Cytokeratin 20: a new marker for early detection of bladder cell carcinoma? J. Urol., *160:* 1971–1974, 1998.

13. Bostick, P. J., Chatterjee, S., Chi, D. D., Huynh, K. T., Giuliano, A. E., Cote, R., and Hoon, D. S. Limitations of specific reverse-transcriptase polymerase chain reaction markers in the detection of metastases in the lymph nodes and blood of breast cancer patients. J. Clin. Oncol., *16:* 2632–2640, 1998.

14. Chausovsky, G., Luchansky, M., Figer, A., Shapira, J., Gottfried, M., Novis, B., Bogelman, G., Zemer, R., Zimlichman, S., and Klein, A. Expression of cytokeratin 20 in the blood of patients with disseminated carcinoma of the pancreas, colon, stomach, and lung. Cancer (Phila.), *86:* 2398–2405, 1999.

15. Fujii, Y., Kageyama, Y., Kawakami, S., Kihara, K., and Oshima, H. Detection of disseminated urothelial cancer cells in peripheral venous blood by a cytokeratin 20-specific nested reverse transcriptase-polymerase chain reaction. Jpn. J. Cancer Res., *90:* 753–757, 1999.

16. Kawamata, H., Uchida, D., Nakashiro, K., Hino, S., Omotehara, F., Yoshida, H., and Sato, M. Haematogenous cytokeratin 20 mRNA as a predictive marker for recurrence in oral cancer patients. Br. J. Cancer., *80:* 448–452, 1999.

17. Soeth, E., Roder, C., Juhl, H., Kruger, U., Kremer, B., and Kalthoff, H. The detection of disseminated tumor cells in bone marrow from colorectal-cancer patients by a cytokeratin-20-specific nested reverse-transcriptase-polymerase-chain reaction is related to the stage of disease. Int. J. Cancer, *69:* 278–282, 1996.

18. Weitz, J., Kienle, P., Magener, A., Koch, M., Schrodel, A., Willeke, F., Autschbach, F., Lacroix, J., Lehnert, T., Herfarth, C., and von Knebel Doeberitz, M. Detection of disseminated colorectal cancer cells in lymph nodes, blood and bone marrow. Clin. Cancer Res., *5:* 1830–1836, 1999.

19. Weber, T., Lacroix, J., Weitz, J., Amnan, K., Magener, A., Holting, T., Klar, E., Herfarth, C., and von Knebel Doeberitz, M. Expression of cytokeratin 20 in thyroid carcinomas and peripheral blood detected by reverse transcription polymerase chain reaction. Br. J. Cancer, *82:* 157–160, 2000.

20. Champelovier, P., Mongelard, F., and Seigneurin, D. CK20 gene expression: technical limits for the detection of circulating tumor cells. Anticancer Res., *19:* 2073–2078, 1999.

21. Bustin, S. A., Gyselman, V. G., Williams, N. S., and Dorudi, S. Detection of cytokeratins 19/20 and guanylyl cyclase C in peripheral blood of colorectal cancer patients. Br. J. Cancer, *79:* 1813–1820, 1999.

22. Wharton, R. Q., Jonas, S. K., Glover, C., Khan, Z. A., Klokouzas, A., Quinn, H., Henry, M., and Allen-Mersh, T. G. Increased detection of circulating tumor cells in the blood of colorectal carcinoma patients using two reverse transcription-PCR assays and multiple blood samples. Clin. Cancer Res., *5:* 4158–4163, 1999.

23. Yun, K., Merrie, A. E., Gunn, J., Phillips, L. V., and McCall, J. L. Keratin 20 is a specific marker of submicroscopic lymph node metastases in colorectal cancer: validation by K-RAS mutations. J. Pathol., *191:* 21–26, 2000.

24. Hu, X. C., and Chow, L. W. Fine needle aspiration may shed breast cells into peripheral blood as determined by RT-PCR. Oncology, *59:* 217–222, 2000.

25. Bae, J. W., Choi, K. H., Kim, H. G., and Park, S. H. The detection of circulating breast cancer cells in peripheral blood by reverse transcriptase-polymerase chain reaction. J. Korean Med. Sci., *15:* 194–198, 2000.

26. Zemer, R., Fishman, A., Bernheim, J., Zimlichman, S., Markowicz, O., Altaras, M., and Klein, A. Expression of cytokeratin-20 in endometrial carcinoma. Gynecol Oncol., *70:* 410–413, 1998.

27. Fishman, A., Klein, A., Zemer, R., Zimlichman, S., Bernheim, J., Cohen, I., and Altaras, M. M. Detection of micrometastasis by cytokeratin-20 (reverse transcription polymerase chain reaction) in lymph nodes of patients with endometrial cancer. Gynecol. Oncol., *77:* 399–404, 2000.

28. Freeman, W. M., Walker, S. J., and Vrana, K. E. Quantitative PCR: pitfalls and potential. Biotechniques, *26:* 112–122, 1999.

29. Wittwer, C. T., Hermann, M. G., Moss, A. A., and Rasmussenn, R. P. Continuous fluorescence monitoring of rapid cycle DNA amplification. Biotechniques, *22:* 130–138, 1997.

30. Wittwer, C. T., Ririe, K. M., Andrew, R. V., David, D. A., Gundry, R. A., and Balis, U. J. The LightCycler: a microvolume multisample fluorimeter with rapid temperature control. Biotechniques, *22:* 176–181, 1997.

31. van Eekelen, J. A., Shammas, F. V., Wee, L., Heikkila, R., and Osland, A. Quantitative analysis of cytokeratin 20 gene expression using RT-PCR and capillary electrophoresis with fluorescent DNA detection. Clin. Biochem., *33:* 457–464, 2000.

32. Funaki, N. O., Tanaka, J., Sugiyama, T., Ohshio, G., Nonaka, A., Yotsumoto, F., Furutani, M., and Imamura, M. Perioperative quantitative analysis of cytokeratin 20 mRNA in peripheral venous blood of patients with colorectal adenocarcinoma. Oncol. Rep., *7:* 271–276, 2000.

33. Futamura, M., Takagi, Y., Koumura, H., Kida, H., Tanemura, H., Shimokawa, K., and Saji, S. Spread of colorectal cancer micrometastases in regional lymph nodes by reverse transcriptase-polymerase chain reactions for carcinoembryonic antigen and cytokeratin 20. J. Surg. Oncol., *68:* 34–40, 1998.

34. Rosenberg, R., Hoos, A., Mueller, J., and Nekarda, H. Impact of cytokeratin-20 and carcinoembryonic antigen mRNA detection by RT-PCR in regional lymph nodes of patients with colorectal cancer. Br. J. Cancer, *83:* 1323–1329, 2000.

Clinical Cancer Research

Quantitative Reverse Transcription-Polymerase Chain Reaction Detection of Cytokeratin 20 in Noncolorectal Lymph Nodes

Richie Soong, Kurt Beyser, Oliver Basten, et al.

Clin Cancer Res 2001;7:3423-3429.